Journal Name

ARTICLE

Novel gold(I) diphosphine-based dimers with aurophilicity-triggered multistimuli light-emitting properties

Received 00th January 20xx,

Accepted 00th January 20xx

DOI: 10.1039/x0xx00000x

www.rsc.org/

Csaba Jobbágy,[a] Péter Baranyai,[a] Gábor Marsi,[a] Barbara Rácz,[a] Liang Li,[b] Panče Naumov*[b] and Andrea Deák*[a]

We report a design strategy for preparation of stimuli-responsive materials with multicolour emission that is based on a single type of luminophore molecule comprising gold(I) and flexible diphosphine ligand. The multistimuli-responsive luminescent dinuclear $[Au_2(dpephos)_2](X)_2$ (dpephos = bis(2-diphenylphosphino)-phenyl ether; X = NO_3, **1**; CF_3SO_3, **2**; BF_4, **3**; PF_6, **4**; SbF_6, **5**) complexes were obtained by rapid mechanochemical syntheses. The single crystal X-ray diffraction analysis of complexes **1**–**5** revealed that the $[Au_2(dpephos)_2]^{2+}$ cations do not exhibit short intramolecular aurophilic interaction. Supported by the structural flexibility of the dpephos ligand, these intramolecular Au···Au contacts are highly sensitive to external stimuli, such as light, temperature, mechanical grinding and exposure to solvent vapours. The ensuing materials, which comprise only gold(I)-diphosphine luminophores, can emit green, yellow and red or red colour, and the colour of the emitted light can be switched by light, heat or pressure. A change from green to yellow in the emission was observed upon heating to room temperature under the excitation with 365 nm, whereas a change from yellow to red was achieved by mechanical grinding. Moreover, the green emission can be switched to red by changing the excitation wavelength to 312 nm. All these reversible luminescence colour changes are readily perceivable by naked eye, and they are attributed to small structural modifications induced by external stimuli that also modulate the intramolecular Au···Au interaction. The red emission from these gold(I) diphosphine-based dimers can be attributed to the presence of intramolecular aurophilic interaction.

Introduction

Biogenic molecular machines utilize external stimuli to elicit structural reconfiguration in response to external effectors such as changes in temperature, pH and gradients in specific small molecules.[1] These biomolecules continue to inspire the development of thermo-, photo-, mechano- and chemoresponsive materials.[2] Although stimuli-responsive materials are not uncommon, the majority of these structures respond to a single stimulus.[2] Along with the recent efforts to develop generic and effective strategies to multi-controllable functional materials,[3] of particular interest to photonic applications are photoluminescent materials whose emission can be switched between different colours by multiple stimuli.[4] However, only a few luminescent materials based on a single type of luminophore molecule that display stimuli-responsive multicolour emission have been reported to date.[5] It remains a great challenge to develop materials constructed from a single type of luminophore molecule that emit more than two distinct colours in response to external stimuli.[5] Mechanochemical approaches continues to gain significance for its application to the development of novel organic and metallosupramolecular solids with desired functional properties.[6] Moreover, whereas reliable mechanochemical strategies have been developed to design and construct porous MOFs with gas sorption behaviour,[6a–c] the construction of luminescent metallosupramolecules[6d,10c] still presents a challenge.

To attain strong luminescence, it is necessary to close the nonradiative relaxation pathways (rotations, vibrations, etc.) of the excited molecules. In general, enhanced emission can be achieved by increasing the molecular rigidity (decreased molecular flexibility), which prevents energy dissipation through the nonradiative relaxation pathways.[7] In contrast, stimuli-responsive luminescence often requires flexible molecular conformations that can be altered by external physical or chemical stimuli.[8] Molecular flexibility becomes an emerging strategy in the design of stimuli-responsive material properties,[9] whereas systematic structural modification of the ligands has been demonstrated to be effective in tuning the emission energy.[10] Specifically, dinuclear complexes $[Au_2(diphos)_2](X)_2$ with a diphosphine ligand (diphos, Chart 1) having short intramolecular aurophilic Au···Au interactions are a remarkable class of materials where the structural diversity of the ligand accounts for the tunability of their emission energy.[10] Within this context we have previously studied the photophysical properties of two complexes, $[Au_2(xantphos)_2](X)_2$ (xantphos = 9,9'-dimethyl-4,5-

[a] Hungarian Academy of Sciences, MTA TTK SZKI, "Lendület" Supramolecular Chemistry Research Group, 1117 Budapest, Magyar Tudósok körútja 2, Hungary; E-mail: deak.andrea@ttk.mta.hu

[b] New York University Abu Dhabi, P.O. Box 129188, Abu Dhabi, United Arab Emirates; E-mail: pance.naumov@nyu.edu

† Electronic Supplementary Information (ESI) available: Experimental details and additional figures. CCDC 1472198-1472203. See DOI: 10.1039/x0xx00000x

bis(diphenylphosphino)-xanthene, Chart 1) and $[Au_2(nixantphos)_2](X)_2$ (nixantphos = 4,6-bis(diphenylphosphino)phenoxazine, Chart 1), and their relation to the nature of the substituents (Me_2C versus NH).[9] In these dinuclear gold(I)-diphosphine compounds, the triplet intraligand transition of the bridging diphosphine ligands occurs at much higher energy than the triplet metal-centered transition originating from an Au···Au interaction.[11] These xantphos- and nixantphos-based $[Au_2(diphos)_2](X)_2$ complexes have stimuli-responsive emission as their luminescence can be switched by temperature, mechanical grinding and solvent vapors.[10a-d] However, their emission can only be switched between two distinct colours. Moreover, excitation-energy-dependent multicolour emission has not been observed with these materials. Better understanding of the luminescent properties of metal complexes can be accomplished by introducing systematic internal (ligands and anions) and external (physical and chemical) variations, and appears as a more elegant strategy for molecular design that allows to exert additional control over their light emission.

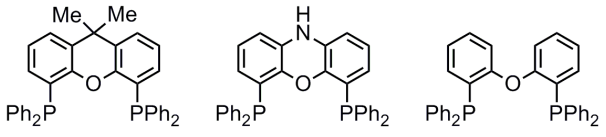

Chart 1

Recently, we summarized the role of noncovalent interactions in the context of the stimuli-responsive behaviour of gold(I) complexes in a review article.[10e] The importance of non-covalent (aurophilic Au···Au, hydrogen bonding, π···π) interactions on structures and luminescent properties of these dinuclear gold(I)-diphosphines has also been recognized.[10a-d] Subtle external changes can perturb the relatively weak aurophilic interactions and can thereby affect the triplet metal-metal (^{3}MM) and metal-metal-to-ligand charge-transfer (^{3}MMLCT) transitions involved in the luminescent emissions.[12] According to previous results,[13,14] the aurophilic interactions can be modulated by temperature, light, pressure and solvent vapours which results in enhanced Au···Au interactions and strongly red-shifted emission.[12] As a recent example, Ito and the co-workers have shown by extensive studies of gold(I) isocyanides that the formation, shortening or breaking of aurophilic bonds can be accomplished by using mechanical force or by photoexcitation, resulting in switching of the photoluminescence.[14]

Motivated by these previous findings, our efforts have been focused on modulation of the intramolecular Au···Au interaction in $[Au_2(diphos)_2](X)_2$ complexes that would allow control of luminescence in the solid state and lead to qualitatively different response to external stimuli. Our previous reports showed that the rigid xantphos- and nixantphos bridging ligands enforce short intramolecular Au···Au distances of ca. 2.8 Å between the gold(I) centers.[10] With this knowledge at hand, we used the more flexible dpephos ligand (dpephos = bis(2-diphenylphosphino)-phenyl ether, Chart 1), in anticipation that its dinuclear $[Au_2(dpephos)_2](X)_2$ complexes can adopt less strained, more flexible conformation having intramolecular Au···Au contact longer (> 2.8 Å) than those observed in the xantphos- and nixantphos-based structures. Moreover, being supported by the structural flexibility of the dinuclear $[Au_2(dpephos)_2]^{2+}$ cation, the intramolecular Au···Au interaction in the ground and/or excited states can be very sensitive to specific external stimuli.

The solid-state mechanochemical approach, in comparison to conventional solution-based techniques,[10f,g] has been proved to be a fast, simple, and efficient route to the synthesis of gold(I)-diphosphine systems that show stimuli-responsive photoluminescent properties. Herein, we report the first stimuli-responsive dinuclear gold(I) system having intramolecular Au···Au separation >3.5 Å that displays aurophilicity-triggered multicolour emission. We present a successful strategy towards new gold(I)-diphos materials that exhibit aurophilicity-triggered unusual stimuli-responsive multicolour luminescence and show three distinct emission colours (green, yellow and red) which can be switched by light, thermal and mechanical stimuli. Moreover, to our knowledge, this also is the first report on multistimuli-responsive luminescent gold(I) complexes that display excitation-energy-dependent emission in the solid state.

Experimental section

Dichloromethane-assisted mechanochemical synthesis of 1

The reaction was carried out by ball-milling stoichiometric amounts of $(Me_2S)AuCl$ (177 mg, 0.6 mmol) and dpephos (323 mg, 0.6 mmol) in the presence of 50 µL dichloromethane for 5 minutes. Next, the as-resulting mixture was further reacted with stoichiometric amounts of $AgNO_3$ (102 mg, 0.6 mmol) in the presence of 50 µL dichloromethane for additional 5 minutes. The crude product was dissolved in dichloromethane (40 mL) and filtered through Celite. The as-resulting clear solution was then precipitated with diethyl ether. **1** was isolated by filtration, washed with diethyl ether and dried under vacuum.

Dichloromethane-assisted mechanochemical synthesis of $[Au_2(dpephos)_2](X)_2$ (X = CF_3SO_3, 2; BF_4, 3; PF_6, 4; and SbF_6, 5) complexes

The dichloromethane-assisted mechanochemical anion-exchange reaction was carried out by ball-milling compound **1** (239 mg, 1.5 mmol) with NaX (X = CF_3SO_3, BF_4, PF_6, and SbF_6) salts in a 1:3 molar ratio (50% excess) with addition of 60 µL dichloromethane for 5 minutes. The mechanochemical reactions produce a powder mixture which was dissolved in dichloromethane (10 mL) and filtered through Celite. The as-resulting clear solution was then precipitated with diethyl ether. The pure anion-exchanged **2**–**5** complexes were isolated by filtration, washed with diethyl ether and dried under vacuum. Recrystallization by slow diffusion of diethyl ether into a

dichloromethane solution of corresponding complexes followed by vacuum drying at room temperature afforded colourless crystals of **1**–**5**. These crystals were utilized in the optical spectroscopic studies of unground solid samples. The ground samples were obtained by mechanical grinding of crystals of **1**–**5** in an agate mortar. For detailed characterization of these unground and ground solids see the Supporting Information.

General Procedures and Physical Measurements

All chemicals and solvents used for the syntheses were of reagent grade. The solvents for synthesis were used without further purification. All manipulations were performed in air. Mechanochemical reactions were performed by a Retsch MM400 shaker mill in a 10 mL agate jar with two 10 mm diameter agate balls operating at 25 Hz.

The mass spectrometry was performed with a Waters QTOF Premier instrument (Waters, Milford, MA, USA) equipped with electrospray ionization source (Waters, Milford, MA, USA) used in the positive ion mode. Mass spectra were recorded using the software MassLynx 4.1 (Waters, Milford, MA, USA) in the mass range 1000–2000 *m/z*. Infrared spectra were recorded in the 400 to 4000 cm^{-1} spectral range on a Varian 2000 FT-IR spectrometer equipped with Golden Gate single reflection diamond ATR (Specac Ltd.). Powder diffractograms were produced with Cu-K_α radiation on a vertical high-angle Philips PW 1050 powder diffractometer. Optical micrographs were recorded with a LINKAM Imaging Station microscope equipped with Nikon DS-Fi1c digital camera and 365 and 312 nm hand-held UV lamps (2×8 W). The movie was recorded on a Nikon D5100 digital camera.

NMR experiments were carried out on Varian Inova (400 MHz for ^1H) and Varian NMR SYSTEM (600 MHz for ^1H) spectrometers using a switchable broadband X{^1H}, and an inverse detection triple tuneable pfg 5mm $^1H^{13}C\{X\}$ probe (X = ^{31}P) respectively. Samples were placed into 5 mm NMR tube and the measuring temperature was 25 °C. ^1H chemical shifts are referenced to the residual solvent signal (CD_2Cl_2: 5.32 ppm). ^{31}P shifts are given relative to the external reference 85% H_3PO_4. Deuterated (99.98 atom%) solvent was purchased from Merck® GmbH, Germany. ^1H spectra were recorded with 16 seconds, while the ^{31}P spectra with 12 seconds relaxation delay and WALTZ-16 proton decoupling. The UV–VIS spectra in methanol were measured on an Agilent 8452A photodiode array spectrometer.

Steady state and time-resolved luminescence measurements were carried out on an Edinburgh Instrument FLSP920 spectrofluorimeter. Spectral corrections were applied using excitation and emission correction functions of the instrument. Longpass filters were used to exclude the scattered excitation light. The solid-state luminescence studies at room temperature were conducted on crystals of **1**–**5** placed in a closed quartz capillary tube. Low temperature (77 K) measurement of crystals of **1**–**5** were carried out by immersing the capillary in a quartz-walled Dewar flask filled with liquid nitrogen. Individual single crystals of **1**–**5** and **1R** were placed on the wall of closed fluorescence cuvette for measuring the room temperature photoluminescence. The solution phase emission measurements were recorded in glassy MeOH:EtOH (4:1) matrix at low temperature in liquid nitrogen (77 K). The excitation light source was a µF900H xenon flashlamp (pulse duration: 2 µs at FWHM) for the luminescent lifetime measurements. In solid state, the absolute measurements of photoluminescence quantum yields were determined according to the literature.[3h] in a calibrated integrating sphere with Spectralon inner surface coating (Thorlabs Instrument) at room temperature. KBr powder was used as a scattering material at the excitation wavelength. The measured scattered and luminescence spectra were corrected according to the relative response of the detector as a function of the wavelength. The quantum yield was calculated by the number of photons emitted divided by the number of photons absorbed. The calculation of the number of photons (the integration of the spectral bands) and the quantum yield were carried out by the F900 spectrometer operating software (Edinburgh Instruments).

Results and discussion

Synthesis and characterization

Complexes of formula $[Au_2(dpephos)_2](X)_2$, X = NO_3 (**1**), CF_3SO_3 (**2**), BF_4 (**3**), PF_6 (**4**) and SbF_6 (**5**) were prepared by rapid solvent-assisted mechanochemical method developed by us for the synthesis of dinuclear gold(I) diphosphines.[9] The starting complex $[Au_2(dpephos)_2](NO_3)_2$ (**1**) was obtained in high yield by ball-milling equimolar amounts of $(Me_2S)AuCl$ with dpephos and $AgNO_3$. Anion exchange was carried out by ball-milling **1** with NaX (X = CF_3SO_3, BF_4, PF_6 and SbF_6) in a 1:3 molar ratio with addition of few drops of dichloromethane. The solvent-assisted mechanochemical anion-exchange reactions afforded pure $[Au_2(dpephos)_2](X)_2$ complexes, where X = CF_3SO_3 (**2**), BF_4 (**3**), PF_6 (**4**) or SbF_6 (**5**), in high yield. The products were characterized by IR, UV-VIS, ^1H and ^{31}P NMR spectroscopy, MS ESI spectrometry and single crystal X-ray diffraction. The ^{31}P NMR spectra of complexes **1**–**5** reveal that these complexes are dinuclear in CD_2Cl_2, as their spectra contain the characteristic broadened singlet at 32.1 ppm. As for other reported dinuclear gold(I) diphosphines,[10] this line broadening of the ^{31}P NMR resonance revealed the conformational flexibility of the $[Au_2(dpephos)_2]^{2+}$ ion in solution. The dinuclear structure of complexes **1**–**5** was confirmed by MS ESI spectrometry, which showed signal for the $\{[Au_2(dpephos)_2]X\}^+$ (*m/z* 1532.24 for **1**, 1619.20 for **2**, 1557.27 for **3**, 1615.22 for **4**, and 1705.15 for **5**).

Crystal structures

By slow diffusion of diethyl ether into solutions of complexes **1**–**5** in dichloromethane single crystals were obtained and their crystal structures were determined. All complexes crystallize

Journal Name

ARTICLE

Table 1 Selected bond lengths (Å), bond angles (°) and torsion angles (°) in complexes **1**–**5**

	1	**2**	**3**	**4**	**5**
Au(1)–P(1)	2.338(1)	2.337(2)	2.333(2)	2.337(2)	2.341(2)
Au(1)–P(3)	2.333(1)	2.339(2)	2.334(2)	2.339(2)	2.336(2)
Au(2)–P(2)	2.310(1)	2.313(2)	2.314(2)	2.311(2)	2.313(2)
Au(2)–P(4)	2.309(1)	2.317(2)	2.314(2)	2.311(2)	2.310(2)
Au(1)···Au(2)	3.609(2)	3.762(2)	3.546(2)	3.717(2)	3.726(2)
P(1)–Au(1)–P(3)	168.16(2)	165.62(4)	165.24(7)	166.27(4)	165.87(4)
P(2)–Au(2)–P(4)	164.89(2)	171.76(4)	165.87(7)	169.51(4)	170.76(4)
P(1)–C(1)–C(8)–P(2)	53.0(2)	52.3(2)	53.4(2)	53.1(2)	55.7(2)
P(3)–C(13)–C(20)–P(4)	58.2(2)	58.3(2)	53.9(2)	55.7(2)	51.8(2)
P(1)–P(3)–P(4)–P(2)	65.9(2)	65.3(2)	67.7(2)	66.6(2)	65.0(2)
P(1)–Au(1)–Au(2)–P(2)	78.4(2)	72.9(2)	75.7(2)	74.1(2)	77.8(2)
P(3)–Au(1)–Au(2)–P(4)	77.5(2)	77.6(2)	79.8(2)	78.6(2)	73.4(2)
P(1)–Au(1)–Au(2)–P(4)	–101.3(2)	–107.3(2)	–103.7(2)	–106.0(2)	–101.6(2)
P(3)–Au(1)–Au(2)–P(2)	–102.9(2)	–102.1(2)	–100.8(2)	–101.2(2)	–107.1(2)

with one molecule of CH_2Cl_2 in the asymmetric unit. Table 1 contains selected bond lengths, bond angles and torsion angles. As shown in Figure 1, the crystal structures of complexes **1**–**5** contain a similar $[Au_2(dpephos)_2]^{2+}$ unit, that incorporates two gold centres and two bridging dpephos ligands. The cationic $[Au_2(dpephos)_2]^{2+}$ core consists of 16-membered metallacycle in a twist-boat conformation (Figure S21).

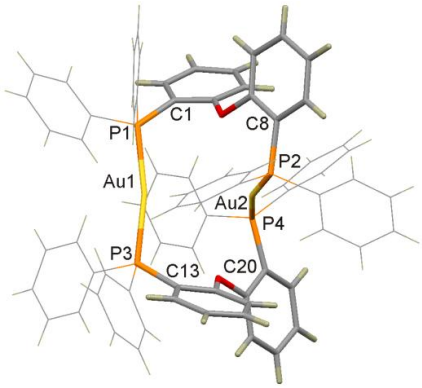

Fig. 1 Cationic $[Au_2(dpephos)_2]^{2+}$ skeleton in complexes **1**–**5**. Colour scheme: gold, yellow; phosphorous, orange; carbon, grey; oxygen, red; hydrogen, dark brown. The phenyl groups are shown as a wireframe model.

In complexes **1**–**5**, the twist induced in the bridging diphenyl ether backbone can be described by the torsion angles P(1)–C(1)–C(8)–P(2) and P(3)–C(13)–C(20)–P(4), which range from 51.8 to 58.3° (Table 1). Significantly smaller torsion angles (19.8–35.1°) have been observed in the less flexible xantphos- and nixantphos-based $[Au_2(diphos)_2](X)_2$ complexes that enforce short intramolecular Au···Au distances of ca. 2.8 Å and display figure-eight conformation.[10] In contrast, there are no significant intramolecular Au···Au interaction in $[Au_2(dpephos)_2]^{2+}$ cations (**1**–**5**). The Au···Au distance ranges from 3.55 to 3.76 (Table 1), which is somewhat longer than the distance of 3.50 Å which is typically considered the upper limit for aurophilic interactions.[15]

Overall, as it was expected these dinuclear gold(I) complexes **1**–**5** based on bridging dpephos ligands adopt a less strained and more flexible conformation and exhibit significantly longer Au···Au distances than the xantphos- and nixantphos-based derivatives. It should be noted that there are additional short C–H···O (**1** and **2**) and C–H···F (**2**–**5**) contacts between the $[Au_2(diphos)_2]^{2+}$ cations and anions, as well as, short C–H···O (**1** and **2**) and C–H···F (**3**–**5**) contacts between the dichloromethane molecules and anions.

Photophysical properties and response to stimuli

Photophysical properties in solution

The UV-Vis absorption spectra of complexes **1**–**5** and the free dpephos ligand in methanol are shown in Figure 2. Practically no dependence of the absorption spectra on the counter-ion could be observed, indicating that there is no interaction between the $[Au_2(dpephos)_2]^{2+}$ cation and the counter-anions

in dilute methanolic solution. The absorption spectra of complexes **1**–**5** are somewhat red-shifted in comparison with the spectrum of the free ligand. The absorption band below 250 nm is also found in the free dpephos ligand and is attributed to the IL (intraligand π → π*) transitions within the diphenyl ether moiety and phenyl rings. Arylphosphine molecules generally exhibit an intense UV transition near 270 nm which involves promotion of an electron from the lone pair orbital (l) on the phosphorus atom to an empty π* orbital of a phenyl ring connected to the phosphorus atom.[16] Therefore, the lowest energy band at 265 nm in the absorption spectrum of the free ligand can be assigned to l → π* transition.

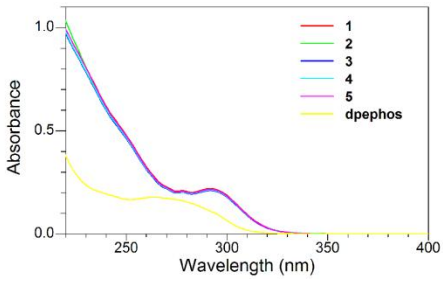

Fig. 2 Absorption spectra of complexes **1**–**5** and dpephos in methanol (10 μM).

Based on DFT calculations (M06/LANL2DZ)[17] on the optimized singlet ground state structure of $[Au_2(dpephos)_2]^{2+}$ cation and TD DFT analysis, the lowest energy absorption band (λ = 295 nm) is assigned to the transition between the highest occupied molecular orbital and the lowest unoccupied molecular orbital (HOMO → LUMO, λ_{calc} = 291 nm, f (oscillator strength) = 0.022; Table S2). The HOMO is localized mainly on the dpephos ligands, whereas the LUMO is located on the phosphorous and gold atoms (Figure S22).

The methanol solution of complexes **1**–**5** was non-emissive at 298 K. This is in accordance with our previous results obtained for dinuclear $[Au_2(diphos)_2](X)_2$ complexes, that show that the solution-state luminescence is quenched by the twisting motion of structurally flexible $[Au_2(diphos)_2]^{2+}$ cations.[10f] In contrast, however, as shown in Figure 3, a structureless band with a maximum at 628 nm developed upon excitation with 290 nm in a glassy matrix (MeOH:EtOH, 4:1) at 77 K. The emission spectra of all complexes **1**–**5** were not affected by the excitation wavelength. The similarity between the excitation (Figure 3) and absorption spectra (Figure 2) indicates that the luminescence in glassy matrix originates from individual $[Au_2(dpephos)_2]^{2+}$ ions. It is, however, completely consistent with the expectations, that there should be a contraction of intramolecular aurophilic Au···Au distance with decreasing temperature. Moreover, the large Stokes shift between the absorption and emission bands, as well as, the long lifetime of 176 μs suggest that the low-energy emission centred at 628 nm could be related to intramolecular aurophilic Au···Au interaction present in the excited triplet state of $[Au_2(dpephos)_2]^{2+}$ cation.[18]

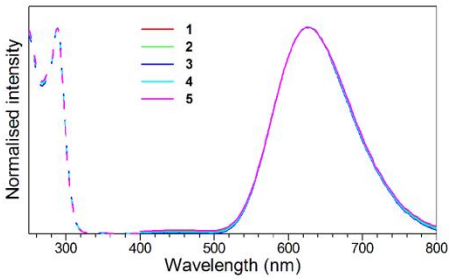

Fig. 3 Emission (λ_{ex} = 290 nm, solid lines) and excitation (λ_{em} = 628 nm, dashed lines) spectra of complexes **1**–**5** in glassy matrix (MeOH:EtOH, 4:1) at 77 K.

Photophysical properties in the solid state

Excitation-wavelength dependent and thermochromic luminescence

As shown in Figure 4a, crystals of **5** exhibit green, crystals of **2**–**4** greenish-yellow, crystals of **1** yellow luminescence upon excitation at 365 nm at room temperature (RT). Upon excitation with a 312 nm UV lamp (Figure 4b), the crystals exhibited orange (**4** and **5**) and red (**1**, **2** and **3**) luminescent colours at RT.

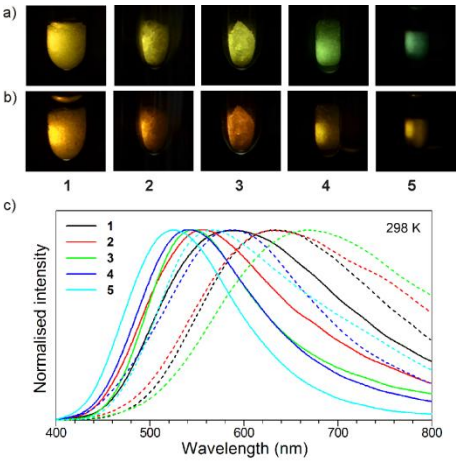

Fig. 4 Optical images of crystals of **1**–**5** taken under 365 nm (a) and 312 nm (b) UV lamp and (c) excitation wavelength-dependent emission spectra of crystals of **1**–**5** at 298 K (λ_{ex} = 365 nm, solid lines; λ_{ex} = 312 nm, dashed lines).

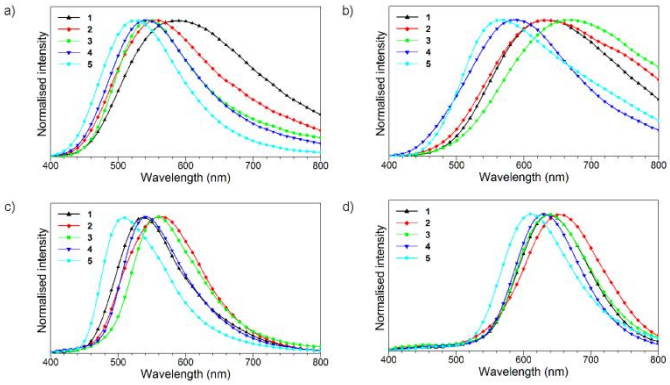

Fig. 5 Emission spectra of crystals of **1**–**5** upon excitation with 365 nm (a) and 312 nm (b) at 298 K and 365 nm (c) and 312 nm (d) at 77 K, respectively.

As shown in Figure 4c, the emission spectra of crystals of **1**–**5** show broad high-energy (HE) emission band ranging from 526 to 590 nm upon 365 nm excitation (Figure 5a, Table 2), however, red-shifted low-energy emission bands (LE) centred between 568–668 nm were detected upon 312 nm excitation at 298 K (Figure 5b, Table 2).

Upon lowering of the temperature to 77 K, green (**1**, **3**–**5**) or yellow (**2**) emission was observed upon excitation at 365 nm (Figure 6a), while bright orange (**5**) and red (**1**–**4**) emissions were observed upon 312 nm excitation (Figure 6b).

Table 2 Emission maxima (in nm) of HE and LE bands for crystals of **1**–**5** at 298 K and 77 K, respectively

Complex	*T* = 298 K		*T* = 77 K	
	λ_{ex} = 365 nm	λ_{ex} = 312 nm	λ_{ex} = 365 nm	λ_{ex} = 312 nm
1	590	634	539	640
2	558	637	563	654
3	547	668	560	639
4	542	589	542	630
5	526	568	510	613

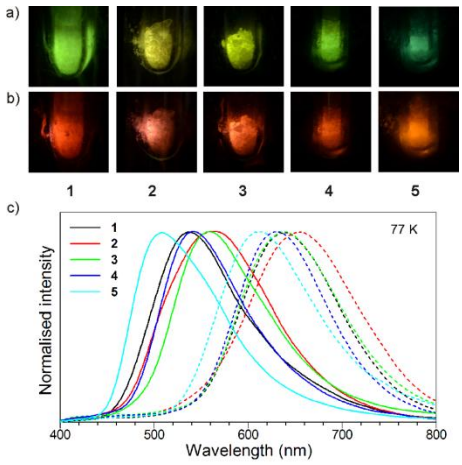

Fig. 6 Optical images of crystals of **1**–**5** taken under 365 nm (a) and 312 nm (b) UV lamp and (c) excitation wavelength-dependent emission spectra of crystals of **1**–**5** at 77 K (λ_{ex} = 365 nm, solid lines; λ_{ex} = 312 nm, dashed lines)

As shown in Figure 6c, narrower bands at 510–563 nm evolved with 365 nm excitation (Figure 5c, Table 2), whereas new emission bands between 613–654 nm developed upon 312 nm excitation (Figure 5d, Table 2) at 77 K.

The emission spectra of crystals of **1**–**5** at both excitation wavelengths (Figures 4c and 6c) are temperature-dependent (Figure 5). We also found that these dinuclear gold(I)-diphosphines exhibit excitation wavelength-dependent tuneable visible emission, and their emission spectrum is characterized by two emission bands of different energy whose ratio depends on the excitation energy. Variation of the excitation wavelength results in a marked change in luminescent colours (Figures 4 and 6), and high-energy and low-energy bands develop in the emission spectra. It is worth noting that excitation wavelength-dependent emission has been observed even for individual single crystals of **1**–**5** (see SI).

As shown in Figure 7, the excitation spectra of all complexes **1**–**5** (Figure S24) corresponding to the HE emission band display a relatively narrow band with a maximum near 365 nm, whereas the LE bands appear across a broad excitation range below 360 nm (Figure S25). Thus, despite the overlap, the two emission bands show distinctly different excitation spectra (Figure 7) and lifetimes (Table 3), indicating poor coupling between the two excited states.

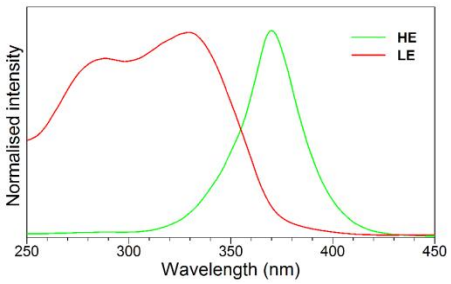

Fig. 7 Typical excitation spectra of complexes **1**–**5** monitoring at the HE and LE bands.

Table 3 Luminescent lifetimes ~~(in μs)~~ of HE (λ_{ex} = 365 nm) and LE (λ_{ex} = 312 nm) bands for complexes **1**–**5** at 298 K and 77 K, and quantum yields at room temperature[a]

Complex	*T* = 298 K			*T* = 77 K		
	τ_{HE} (μs)	Φ_{HE}	τ_{LE} (μs)	Φ_{LE}	τ_{HE} (μs)	τ_{LE} (μs)
1	1.4	0.17	24	0.13	80	136
2	2.8	0.19	21	0.12	26	110
3	3.6	0.18	23	0.12	44	107
4	1.4	0.14	21	0.11	38	111
5	1.2	0.15	21	0.11	35	123

[a] Excitation wavelengths were 365 nm and 312 nm for HE and LE bands, respectively.

These results suggest that the high-energy and low-energy emissions originating from different non-interacting excited states of $[Au_2(diphos)_2]^{2+}$ cations are populated mainly by direct excitation, and the energy transfer between these states is inefficient. A similar behaviour has been observed in other Au(I) complexes showing a strong excitation wavelength-dependent emission.[19a,b,c] Fackler and co-workers reported that the HE and LE emissions of (TPA)AuX (TPA = 1,3,5-triaza-7-phosphaadamantane; X= Br or Cl) complex operates independently and shows substantially different excitation spectra.[19a] They ruled out the presence of two different emitting species since the photoluminescence data were also reproduced on X-ray-quality single crystals.[19a] On the basis of these results, they proposed that the (TPA)AuX system shows multiple emitting states in its solid state structure. In other words, the (TPA)AuX can generate two different excited states, one giving the HE band and the other one giving the LE band upon excitation with different wavelengths.

The HE emission is similar in energy and shape to that of the phosphorescence of the dpephos ligand (Figure S26), resulting from 365 nm excitation. The Stokes shift between the near UV excitation and the HE emission bands is significantly smaller as compared to LE band, which indicates that a slight geometrical change of the $[Au_2(dpephos)_2]^{2+}$ cation exists within this transition. Based on these experimental findings and analogies

in the literature,[19a,b,c] we can tentatively assign the HE and LE bands as due to the formation of two different excited states with somewhat different molecular conformations.

The luminescence lifetimes of the LE bands of complexes **1**–**5** are much longer than those of the respective HE bands (Table 3). The relatively long lifetime of LE bands (Table 3), developed in the emission spectra upon excitation with 312 nm, could facilitate the shortening of the Au···Au distance and formation of stronger aurophilic (Au···Au)* bonding in the excited state.

The quantum yields of **1**–**5** (Table 3) are significantly higher than those of $[Au_2(dcpm)_2](X)_2$ (X = Cl, I, CF_3SO_3, ClO_4, PF_6, and $[Au(CN)_2]$) complexes with flexible bis(dicyclohexylphosphino)-methane (dcpm) (Φ = 0.013–0.085).[12c] They are also higher than those of $[Au_2(diphos)_2](NO_3)_2$ complexes with more rigid xantphos (Φ = 0.024) and nixantphos (Φ = 0.004) ligands. The quantum yields of **1**–**5** (Table 3) are similar to that of $[Au_2(dppm)_2](CF_3SO_3)_2$ (Φ = 0.23) with bis(diphenylphosphino)-methane (dppm), which was effectively used in the fabrication of light-emitting diodes.[4h]

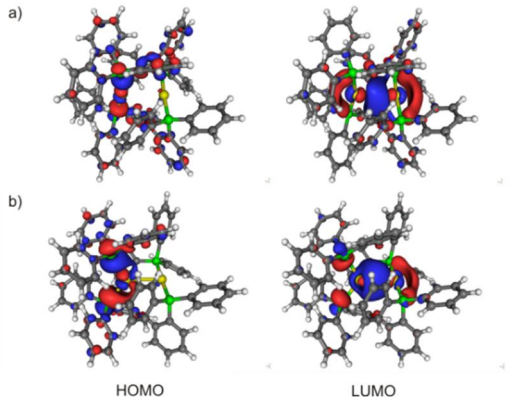

Fig. 8 Contour plots of the HOMO and LUMO superimposed on the a) singlet ground (S_0) and b) triplet excited (T_1) state geometry of $[Au_2(dpephos)_2]^{2+}$.

To further interpret the origin of LE emission, we performed theoretical calculations to assess the Au···Au interaction in the excited state (see SI for computational details). The electronic structure of the lowest excited triplet (T_1) state for $[Au_2(dpephos)_2]^{2+}$ cation was analysed by DFT optimization (UM06/LANL2DZ) and TD DFT computational methods. The 2.942 Å Au···Au distance indicates the formation of aurophilic (Au···Au)* bonding in the T_1 excited state of $[Au_2(dpephos)_2]^{2+}$. According to TD DFT calculation the phosphorescence from T_1 state could be described predominantly (orbital contribution: 87%) as transition between LUMO and HOMO (Figure 8). The calculated emission wavelength (λ_{calc} = 683 nm) is in good agreement with the experimental value measured for the low-energy emission of complexes **1**–**5**.

Tuning metallophilic interactions by light is a very intriguing aspect of the materials described here, however, tunability of the excitation wavelength-dependent emission is rarely observed for luminescent gold(I) compounds.[8e,19] Previous experimental and theoretical works also revealed substantial shortening of both intra- and intermolecular aurophilic interactions upon photoexcitation.[11,20] Resonance Raman study of Che and coworkers showed that the intramolecular Au···Au distance decreases from 2.92 Å in the ground state to 2.80 Å in the first excited state of dinuclear $[Au_2(dcpm)_2](ClO_4)_2$ complex.[11] Recently, Ito and co-workers reported the photoinduced single-crystal-to-single-crystal (SCSC) phase transition of blue-emitting crystals of a gold(I) isocyanide complex into a yellow-emitting polymorph.[20d] Photoinduced shortening of intermolecular Au···Au distance from 3.5041(14) to 3.2955(6) Å occurred during this SCSC transition. Upon UV irradiation, the shape of the broad emission band of blue-emitting crystals with λ_{max} at 448 nm changes dramatically and a new broad emission band with a structureless maximum at 580 nm evolved.[20d]

Mechanochromic luminescence

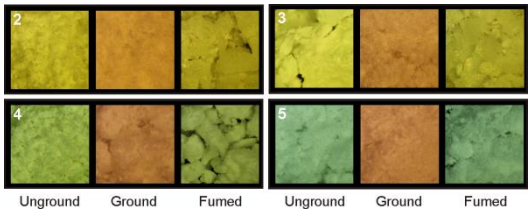

Fig. 9 Optical images taken under 365 nm UV lamp illumination showing the reversible mechanochromic luminescence of complexes **2**–**5** upon grinding and exposure to solvent vapours.

All complexes **1**–**5** exhibit tunable luminescence in the solid state under the effect of external mechanical stimuli and exposure to organic vapours. As shown in Figure 9, complexes **2**–**5** display reversible mechanochromic luminescence.

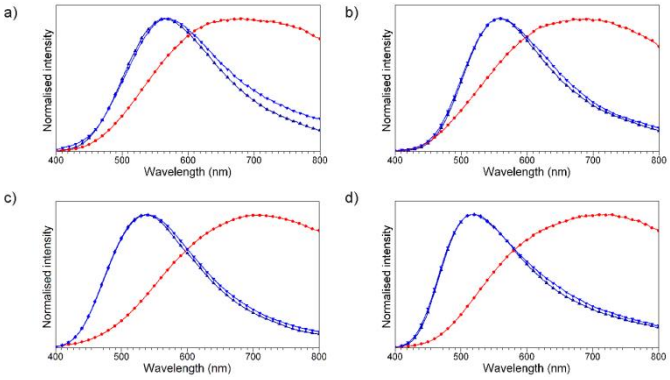

Fig. 10 Emission spectra of unground (dark blue), ground (red) and fumed (blue) forms of complexes **2** (a), **3** (b), **4** (c) and **5** (d) showing the reversible mechanochromic luminescence.

Their green (**5**) and greenish-yellow (**2**–**4**) emission changes to red upon grinding and reverts to the original emission upon exposure to solvent vapours (Figure 10). More surprisingly, the yellow-emitting complex **1** does not exhibit reversible mechanochromic luminescence. Its red emission obtained after mechanical grinding, changes into reddish-orange upon subsequent solvent vapour fuming (Figure 11a).

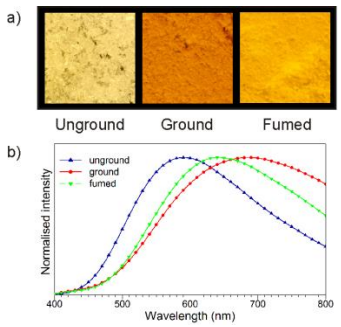

Fig. 11 a) Photographs showing the luminescence colour changes of complex **1** upon mechanical grinding and subsequent solvent treatment and b) the corresponding emission spectra.

The grinding-induced changes in the emission colour correspond to appearance of low-energy bands in the emission spectra of complexes **1**–**5**, as shown in Figure 10 and Figure 11b. Thus, the emission spectra obtained upon excitation with 365 nm display broad low-energy emission bands centered between 683 and 718 nm, and the decay lifetimes of these bands are in the range of ca. 15−19 μs (Table 4). Upon mechanical grinding, the quantum yields of **1**–**5** (Table 3) were considerably lowered to 4–6% (Table 4).

The powder X-ray diffraction (PXRD) patterns of crushed crystals of **1**–**5** agree with the patterns simulated from single crystal diffraction data (see SI). As confirmed by PXRD (see SI), by grinding these crystalline gold(I)-diphosphines are converted into amorphous powders. ^{1}H NMR analysis of unground and ground samples of **1**–**5** showed that the residual solvent molecules were lost during grinding (see details in SI). Upon exposure of the ground phases to CH_2Cl_2 vapour, the PXRD patterns of complexes **2**–**5** restored to the original patterns (SI). The mechanically stimulated changes of the luminescence colour involves crystalline-to-amorphous phase transition typical for dinuclear diphosphine-based $[Au_2(diphos)_2](X)_2$ systems reported by us.[10] The flexibility of the $[Au_2(dpephos)_2]^{2+}$ cations, coupled to a relatively loose molecular packing facilitates the pressure- and shear-induced deformation and can ultimately drive the transformation to amorphous phase accompanied by change in photoluminescence. As a consequence of mechanical grinding, the HE bands disappear and the LE bands become dominant for all compounds. The lifetimes are also extended (Table 4). The luminescence spectral changes induced by mechanical grinding are much smaller upon excitation at 312 nm UV light relative to 365 nm (see SI). The difficulty of structural characterization of amorphous phase is an obstacle to study the external stimuli-triggered structural changes in crystalline-to-amorphous phase transition leading to luminescent responses. However, several reports on mechanochromic luminescent gold(I),[14] copper(I)[21] and platinum(II)[22] complexes attributed the mechanically-induced luminescence changes to shortening of metal···metal bonds, which reinforce the phosphorescence from triplet metal−metal (^{3}MM) states.[21,22] Recently, we also reported grinding-induced aurophilic bond formation in a mechanochemical monomer-dimer conversion of a nixantphos-based Au(I) complex that results in significant luminescence colour swiching.[10d]

Convincing structural evidence of mechanically-induced aurophilic bond formation has been reported to occur upon mechanical pricking of gold(I) isocyanide single crystals, in which drastic shortening of Au···Au distances (from 5.733 to 3.177 Å) leads to luminescence alteration.[14a] Leznoff and co-workers reported the pressure-dependent luminescence of $[Au_2(dopdtc)_2]$ (dopdtc = di(o-pyridyl)aminedithiocarbamate) dimer, whose crystal structure contains two crystallographically inequivalent $[Au_2(dopdtc)_2]$ molecules having intramolecular Au···Au bonds of 2.7932(4) and 2.8161(4) Å, respectively.[14d] These dimers generate a supramolecular 1D chain structure through kinked intermolecular aurophilic interactions of 2.9928(31) Å. The broad emission band of $[Au_2(dopdtc)_2]_n$ indicated that ligand-centered vibrational modes having MLCT character are involved in emission. The previously reported analogous $[Au_2(edtc)_2]_n$ (edtc = diethyldithiocarbamate)[14e] complex with 2.782 Å intra- and 3.004 Å intermolecular Au···Au distance shows typical MM centered transition. This transition leads to narrow emission band (λ_{max} = 550 nm) as the Au−Au vibrational frequencies are low.[14d] However, a broad LE band at 710 nm was observed in the emission spectrum above 30 kbar. Upon application of pressure, the intermolecular Au···Au distances decrease substantially more than other bond lengths, and the band width of $[Au_2(edtc)_2]_n$ at above 30 kbar is comparable to the $[Au_2(dopdtc)_2]_n$ spectrum.[14d] This broadening suggests that the aurophilic chain becomes more kinked with increasing pressure, leading to dominant MLCT luminescence from kinked chain segments of $[Au_2(edtc)_2]_n$. Such MLCT transition was observed at room temperature for $[Au_2(dopdtc)_2]_n$ having kinked aurophilic chain, for which, however, only small pressure-induced shift of the luminescence band maximum and band shape was noticed.[14d] In these systems, the proximity of several different excited states that are close in energy can lead to a different emitting state,[14e] as illustrated by the dominance of a broad emission band at high pressures for $[Au_2(dopdtc)_2]_n$. However, the presence of a weak broader band at HE (~ 710 nm) illustrates that crystal defects leading to sites with this emitting behaviour exist even at ambient pressure.[14e] In another study, Fackler and co-workers attributed the excitation wavelength-dependent blue (λ_{excit} < 360 nm) and green (λ_{excit} > 360 nm) emission of powdered $[(TPA)_2Au][Au(CN)_2]$ complex to defect sites, which were created by mechanical grinding.[14f] It was suggested that the emission from this powdered gold(I) complex originates from lattice defect centres that operate independently with little communication between them.[14f]

Therefore, we can conclude that the LE emission bands in the emission spectra of ground samples of **2**–**5** could be attributed to the contraction of Au···Au distance in amorphous phases.

Table 4 Emission maxima, luminescent lifetimes and quantum yields of complexes **1**–**5** upon grinding and exposure to solvent vapours using 365 nm excitation at room temperature.

Complex	Ground			Fumed		
	λ_{max} (nm)	τ (μs)	Φ	λ_{max} (nm)	τ (μs)	Φ
1	688	18	0.04	640	17	0.14
2	687	19	0.06	570	3.6	0.17
3	683	15	0.05	561	4.1	0.16
4	710	17	0.04	578	2.7	0.13
5	718	16	0.05	519	2.9	0.15

The HE bands recovered in the emission spectra of complexes **2**–**5** (Figure 10) upon exposure to solvent vapours that triggered the crystallization of amorphous phases (see the SI). These compounds demonstrate excellent reproducibility of the mechanochromic luminescent response over four cycles of grinding and treatment with solvent (for details, see the SI). Thus, the luminescent LE band can be reversibly switched into HE band by mechanical/solvent-induced dynamic crystalline-to-amorphous phase transitions. A movie showing the reversible mechanochromic luminescence is included in the SI.

In the case of complex **1**, the LE band blue-shifted from 688 to 640 nm while the long lifetime was retained upon exposure to solvent (Table 4), and broad peaks were observed in the PXRD pattern (Figure S30). Single crystals (**1R**) (Figure 12) were obtained by slow diffusion of diethyl ether into a dichloromethane solution of this reddish-orange luminescent phase. The emission maxima of these crystals of **1R** is at 639 nm.

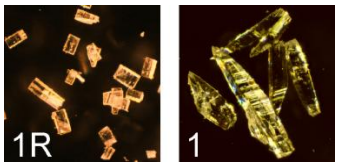

Fig. 12 Optical images recorded under 365 nm UV light showing the crystals of **1R** and **1**.

As shown in Figure 13, the X-ray analysis revealed that the $[Au_2(dpephos)_2]^{2+}$ cation in this reddish-orange **1R** displays intramolecular aurophilic interaction. As a consequence, the twist of the dpephos ligand backbones with respect to the Au···Au axis is somewhat higher than those observed in **1** (Table S11)), whereas there are also some other small variations mainly in bond and torsion angles (see Table S11 in SI). On the basis of the two sets of X-ray crystal data, the intramolecular Au···Au distance in the two structures of the cationic $[Au_2(dpephos)_2]^{2+}$ skeleton are different (3.609(1) Å for **1**; 3.238(1) Å for **1R**). Thus, a shortening of 0.37 Å in intramolecular Au···Au distance is sufficient to induce significant changes in luminescence from yellow to reddish-orange (Figure 12). This is consistent with the appearance of HE emission band in **1R** that can be attributed to the formation of aurophilic interaction.

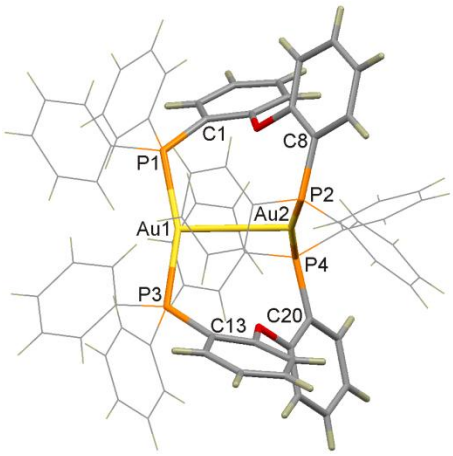

Fig. 13 Cationic $[Au_2(dpephos)_2]^{2+}$ skeleton of complex **1R**. Colour scheme: gold, yellow; phosphorus, orange; carbon, grey; oxygen, red; hydrogen, dark brown. The phenyl groups are shown as a wireframe model.

Potential applications to storing of information

Reversible change in emission colour is an important feature for practical applications. Previously, we demonstrated that the reversible mechanochromic and vapochromic luminescent behaviour of dinuclear gold(I) diphosphines can be utilized in the construction of simple mechano- and vapo-rewritable data recording devices.[10c] In addition to these stimuli-responsive luminescent properties, the newly synthesized gold(I) diphosphines display light-responsive properties, as they could be selectively excited by changing the energy of the excitation. This optically-responsive behaviour is particularly interesting because the stimulus, light, can be applied at highly localized sites without mechanical or physical impact.[23]

Fig. 14 Multicolour fluorescence image of our institutional logo ("ttk") visualized on temperature- and light-responsive microcrystals of **4**.

As shown in Figures 4 and 6, the light-emission of complex **4** can be tuned from yellowish-green to green and orange-red by varying the excitation energy and temperature. As a simple demonstration of the potential applications of the optically-responsive gold(I) dpephos complexes described here, compound **4** was placed in a quartz cuvette and cooled to 77 K. A plastic letter stencil was used as a mask, and the letters "t" and "k" were selected and illuminated with UV light of different wavelengths. Figure 14 shows that orange-red and green-coloured letter "t" can be written by using 312 nm and 365 nm illumination. Moreover, upon heating to room temperature, the yellowish-green "k" letter was visible upon 365 nm illumination. The multicolour luminescence image of the institutional logo "ttk" can be easily produced by changing the excitation wavelength and temperature. This simple experiment based on light- and temperature-triggered reversible multicolour

luminescence variation illustrates a potential applicability in optical devices and sensing applications.

Conclusions

Here we demonstrate a design strategy for multistimuli-responsive materials with multicolour emission properties that is based on a single type of luminophore molecule comprising gold(I) and flexible diphosphine ligand. A series of novel multistimuli-responsive luminescent dinuclear gold(I) complexes of dpephos ligand, $[Au_2(dpephos)_2](X)_2$ (**1**–**5**), has been easily and rapidly prepared by solvent-assisted mechanochemical synthesis. Supported by the structural flexibility of the dpephos ligand, the intramolecular Au···Au contact (3.5–3.8 Å) between the gold(I) centres of the $[Au_2(dpephos)_2]^{2+}$ cation of complexes **1**–**5** is highly sensitive to specific external stimuli. Stimuli, such as temperature, light and mechanical grinding can enhance the aurophilic interaction (< 3.5 Å) leading to drastic luminescence changes. Remarkably, these new gold(I) diphosphine-based compounds **1**–**5** exhibit unusual stimuli-responsive multicolour luminescence and show three distinct emission colours of green, yellow and red, which can be switched by light, thermal and mechanical stimuli. The single crystal X-ray studies of a reddish-orange emitting new form (**1R**) originating from red luminescent amorphous phase of $[Au_2(dpephos)_2](NO_3)_2$ resulting upon mechanical grinding showed that this form contains short intramolecular Au···Au distance of 3.238(1) Å, which is indicative of aurophilic interaction. Crystallographic studies correlated with photophysical properties suggest that a shortening of 0.37 Å in intramolecular Au···Au distance is large enough to induce significant luminescence changes from yellow (**1**) to reddish-orange (**1R**). These results suggest that the red emission of these gold(I)-diphosphine dimers can be attributed to the formation of intramolecular aurophilic interaction triggered by external stimuli. As evidenced by our results, the response to excitation energy, temperature and mechanical stimuli provides a very simple and convenient way to tune the emission colours of these gold(I) diphosphine-based dimers between green, yellow and red. Such multistimuli-responsive photofunctional materials have important potential applications in optical storage and memories, temperature, mechanical and chemical sensors, displacement and deformation detectors, optoelectronic, data recording and display devices. Moreover, the red emission at the long-wavelength (low-energy) end of the visible spectrum, however, suggests a potential applicability of these materials in biomedical imaging and signaling, photodynamic therapy, information security and telecommunications.[24] Our study, however, provides a new direction to the design of single luminophore-based stimuli-responsive luminescent materials that exhibit multicolour emission in response to a variety of physical stimuli.

X-ray Crystallography and Data Collection

X-ray diffraction measurement of complexes **1–5** (Table 5) was performed with Bruker APEX DUO diffractometer with monochromated Mo Kα radiation (λ = 0.71073 Å) and CCD detector. The crystal data of complex **1R** (Table 5) was collected on a Rigaku R-AXIS RAPID image plate diffractometer with monochromated Mo Kα radiation (λ = 0.71075 Å). The structures were deposited at the Cambridge Data Centre and allocated with CCDC 1472198-1472203 numbers.

Journal Name

ARTICLE

Table 5 Summary of X-ray diffraction data for complexes **1**–**5** and **1R**

Complex	**1**	**2**	**3**	**4**	**5**	**1R**
Formula	$C_{72}H_{56}Au_2O_2P_4$, 2(NO_3), (CH_2Cl_2)	$C_{72}H_{56}Au_2O_2P_4$, 2(CF_3O_3S), (CH_2Cl_2)	$C_{72}H_{56}Au_2O_2P_4$, 2(BF_4), (CH_2Cl_2)	$C_{72}H_{56}Au_2O_2P_4$, 2(PF_6), (CH_2Cl_2)	$C_{72}H_{56}Au_2O_2P_4$, 2(SbF_6), (CH_2Cl_2)	$C_{72}H_{56}Au_2O_2P_4$, 2 (NO_3), 3.557 (CH_2Cl_2), (H_2O)
Formula weight	1679.94	1854.06	1729.54	1845.86	2027.44	1915.11
Crystal size [mm]	0.10 × 0.15 × 0.20	0.15 × 0.18 × 0.22	0.18 × 0.20 × 0.31	0.11 × 0.15 × 0.15	0.11 × 0.14 × 0.27	0.15 × 0.18 × 0.22
Colour	colourless	colourless	colourless	colourless	colourless	colourless
Crystal system	monoclinic	monoclinic	monoclinic	monoclinic	monoclinic	monoclinic
Space group	*P* $2_1/c$	*P* $2_1/c$	*P* $2_1/c$	*P* $2_1/c$	*P* $2_1/c$	*P* $\bar{1}$
Temp. (K)	100	100	100	100	100	98
a [Å]	21.848(2)	22.275(3)	21.826(2)	22.214(2)	22.639(2)	12.5913(4)
b [Å]	15.478(2)	16.505(2)	16.073(2)	16.180(2)	16.350(2)	13.4958(4)
c [Å]	19.843(2)	19.910(3)	19.712(2)	19.966(2)	20.121(2)	23.9939(9)
α [°]	90	90	90	90	90	91.744(1)
β [°]	106.460(2)	105.095(2)	106.692(3)	105.740(1)	105.230(1)	101.643(1)
γ [°]	90	90	90	90	90	112.048(1)
V [Å^3]	6435.3(2)	7067.3(2)	6623.8(9)	6906.9(9)	7186.3(9)	3675.9(2)
Z	4	4	4	4	4	2
d_{calc} [Mg/m^3]	1.734	1.742	1.734	1.775	1.874	1.730
μ [mm^{-1}]	4.797	4.445	4.672	4.539	5.054	4.391
F(000)	3304	3640	3384	3608	3896	1887
Index ranges (°)	$-29 \le h \le 29$	$-29 \le h \le 29$	$-23 \le h \le 23$	$-28 \le h \le 29$	$-30 \le h \le 30$	$-15 \le h \le 15$
	$-20 \le k \le 20$	$-21 \le k \le 21$	$-17 \le k \le 17$	$-21 \le k \le 21$	$-21 \le k \le 21$	$-16 \le k \le 16$
	$-26 \le l \le 26$	$-26 \le l \le 26$	$-21 \le l \le 21$	$-26 \le l \le 26$	$-26 \le l \le 26$	$-29 \le l \le 29$
No. of reflections collected	178161	83647	54561	81807	170498	132875
No. of indep. reflns./R_{int}	16016/0.069	17549/0.046	8922/0.079	17176/0.051	17976/0.041	14938/0.049
No. of obsd. reflns. $I > 2\sigma(I)$	13038	13962	6813	13469	15013	12114
No. of parameters	820	896	839	875	884	905
GOOF	1.00	1.01	1.02	1.01	1.03	1.18
*R*1 (obsd. data)	0.0240	0.0336	0.0363	0.0314	0.0302	0.0514
*wR*2 (all data)	0.0455	0.0846	0.0791	0.0685	0.0767	0.1217
Largest diff. peak/hole [eÅ^{-3}]	–0.65/0.67	–3.03/3.22	–1.15/2.75	–1.55/2.23	–2.84/3.79	–1.98/2.50

Acknowledgements

The authors gratefully acknowledge the support by MTA (Hungarian Academy of Sciences) through the Lendület Programme (LP2012-21/2012), this work was carried out partically using Core Technology Platform resources at New York University Abu Dhabi.

Notes and references

1 K. Chockalingam, M. Blenner and S. Banta, *Protein Eng. Des. Sel.*, 2007, **20**, 155–161.

2 (*a*) C. Niu, Y. You, L. Zhao, D. He, N. Na and J. Ouyang, *Chem. Eur. J.*, 2015, **21**, 13983–1399; (*b*) Z. Mao, Z. Yang, Y. Mu, Y. Zhang, Y.-F. Wang, Z. Chi, C.-C. Lo, S. Liu, A. Lien and J. Xu, *Angew. Chem. Int. Ed.*, 2015, **54**, 6270–6273; (*c*) T. Lasanta, M. E. Olmos, A. Laguna, J. M. López-de-Luzuriaga and P. Naumov, *J. Am. Chem. Soc.*, 2011, **133**, 16358–16361; (*d*) A. Laguna, T. Lasanta, J. M. Lopez-de-Luzuriaga, M. Monge, P. Naumov and M.E.Olmos, *J. Am. Chem.Soc.*, 2010, **132**, 456–457; (*e*) E. J. Fernández, J. M. López-de-Luzuriaga, M. Monge, M. E. Olmos, J. Pérez, A. Laguna, A. A. Mohamed and J. P. Fackler, *J. Am. Chem. Soc.*, 2003, **125**, 2022–2023; (f) P. Xue, J. Ding, P. Wang and R. Lu, *J. Mater. Chem. C.*, 2016, **4**, 6688–6706.

3 (*a*) A. J. McConnell, C. S. Wood, P. P. Neelakandan and J. R. Nitschke, *Chem. Rev.*, 2015, **115**, 7729–7793; (*b*) P. K. Kundu, G. L. Olsen, V. Kiss and R. Klajn, *Nat. Commun.*, 2014, **5**, 3588; (*c*) K. Chen, M. M. Nenzel, T. M. Brown and V. J. Catalano, *Inorg. Chem.*, 2015, **54**, 6900–6909; (*d*) J. R. Berenguer, J. Fernández, B. Gil, E. Lalinde and S. Sánchez, *Chem. Eur. J.*, 2014, **20**, 2574–2584; (*e*) P. Chen, Q. Li, S. Grindy and N. Holten-Andersen, *J. Am. Chem. Soc.*, 2015, **137**, 11590–11593; (*f*) J. Mei, N. L. C. Leung, R. T. K. Kwok, J. W. Y. Lam and B. Z. Tang, *Chem. Rev.*, 2015, **115**, 11718–11940; (*g*) R. Li, S. Xiao,

Please do not adjust margins

Y. Li, Q. Lin, R. Zhang, J. Zhao, C. Yang, K. Zou, D. Lia and Tao Yi, *Chem. Sci.*, 2014, **5**, 3922–3928; (*h*) J. C. deMello, H. F. Wittmann and R. H. Friend, *Adv. Mater.,* 1997, **9**, 230–232.

4 (*a*) Y. Sagara and T. Kato, *Nat. Chem.* 2009, **1**, 605–610; (*b*) Z. Chi, X. Zhang, B. Xu, X. Zhou, C. Ma, Y. Zhang, S. Liu and J. Xu, *Chem. Soc. Rev.* 2012, **41**, 3878–3896; (*c*) X. Zhang, Z. Chi, Y. Zhang, S. Liu and J. Xu, *J. Mater. Chem. C* 2013, **1**, 3376–3390; (*d*) H. Sun, S. Liu, W. Lin, K. Y. Zhang, W. Lv, X. Huang, F. Huo, H. Yang, G. Jenkins, Q. Zhao and W. Huang, *Nat. Commun*., 2014, **5**, 3601; (*e*) J. Liang, Z. Chen, L. Xu, J. Wang, J. Yin, G.-A. Yu, Z.-N. Chen and S. H. Liu, *J. Mater. Chem. C* 2014, **2**, 2243–2250; (*f*) X. Zhang, J.-Y. Wang, J. Ni, L.-Y. Zhang and Z.-N. Chen, *Inorg. Chem.*, 2012, **51**, 5569–5579; (*g*) J. Ni, X. Zhang, Y.-H. Wu, L.-Y. Zhang and Z.-N. Chen, *Chem. Eur. J*., 2011, **17**, 1171–1183; (h) Y. Ma, C.-M. Che, H.-Y. Chao, X. Zhou, W.-H. Chan and J. Shen, *Adv. Mater.* 1999, **11**, 852–857.

5 (*a*) Y. Sagara and T. Kato, *Angew. Chem. Int. Ed.*, 2011, **50**, 9128–9132; (*b*) Z. Ma, M. Teng, Z. Wang, S. Yang and X. Jia, *Angew. Chem. Int. Ed.*, 2013, **52**, 12268–12272. (*c*) J.-F. Chen, D.-P. Gong, J. Wen, H. Mab and D.-K. Cao, *Chem. Sci.*, 2016, **7**, 451-456; (*d*) Y. Sagara, S. Yamane, M. Mitani, C. Weder and T. Kato, *Adv. Mater.* 2016, **28**, 1073–1095.

6 (*a*) M. J. Cliffe, C. Mottillo, R. S. Stein, D.-K. Bučar and T. Friščić, *Chem. Sci.*, 2012, **3**, 2495–2500; (*b*) T. Friščić, D. G. Reid, I. Halasz, R. S. Stein, R. E. Dinnebier and M. J. Duer, *Angew. Chem. Int. Ed.* 2010, **49**, 712–715; (*c*) T. D. Bennett, S. Cao, J. C. Tan, D. A. Keen, E. G. Bithell, . P. J. Beldon, T. Friščić and A. K. Cheetham, *J. Am. Chem. Soc.*, 2011, **133**, 14546–14549; (*d*) A. Kobayashi, T. Hasegawa, M. Yoshida and M. Kato, *Inorg. Chem.*, 2016, **55**, 1978–1985; (*e*) N. R. Rightmire and T. P. Hanusa, *Dalton Trans.*, 2016, **45**, 2352–2362.

7 (*a*) J.-H. Jia and Q.-M. Wang, *J. Am. Chem. Soc.*, 2009, **131**, 16634–16635; (*b*) V. V. Sivchik, A. I. Solomatina, Y.-T. Chen, A. J. Karttunen, S. P. Tunik, P.-T. Chou and I. O. Koshevoy, *Angew. Chem. Int. Ed.,* 2015, **54**, 14057–14060.

8 (*a*) E. L. Harty, A. R. Ha, M. R. Warren, A. L. Thompson, D. R. Allan, A. L. Goodwin and N. P. Funnell, *Chem. Commun.*, 2015, **51**, 10608–10611; (*b*) Y. Zhang, J. Sun, G. Zhuang, M. Ouyang, Z. Yu, F. Cao, G. Pan, P. Tang and C. Zhang and Y. Ma, *J. Mat. Chem. C,* 2014, **2**, 195–200; (*c*) P. S. Hariharan, D. Moon and S. P. Anthony, *J. Mat. Chem. C,* 2015, **3**, 8381–8388; (*d*) Y. Lin, G. Chen, L. Zhao, W. Z. Yuan, Y. Zhang and B. Z. Tang, *J. Mat. Chem. C* 2015, **3**, 112–120; (*e*) W.-X. Ni, M. Li, J. Zheng, S.-Z. Zhan, Y.-M. Qiu, S. W. Ng and D. Li, *Angew. Chem. Int. Ed.*, 2013, **52**, 13472–13476; (*f*) B. Xu, J. He, Y. Mu, Q. Zhu, S. Wu, Y. Wang, Y. Zhang, C. Jin, C. Lo, Z. Chi, A. Lien, S. Liua and J. Xu, *Chem. Sci.*, 2015, **6**, 3236-3241.

9 M. R. R. Prabhath, J. Romanova, R. J. Curry, S. R. P. Silva and P. D. Jarowski, *Angew. Chem. Int. Ed.*, 2015, **54**, 7949–7953.

10 (*a*) Cs. Jobbágy, M. Molnár, P. Baranyai, A. Hamza, G. Pálinkás and A. Deák, *CrystEngComm* 2014, **16**, 3192–3202; (*b*) Cs. Jobbágy, M. Molnár, P. Baranyai and A. Deák, *Dalton Trans.* 2014, **43**, 11807–11810; (*c*) A. Deák, Cs. Jobbágy, G. Marsi, M. Molnár, Z. Szakács and P. Baranyai, *Chem. Eur. J.*, 2015, **21**, 11495–11508; (*d*) P. Baranyai, G. Marsi, Cs. Jobbágy, A. Domján, L. Oláh and A. Deák, *Dalton Trans.* 2015, **44**, 13455–13459; (*e*) Cs. Jobbágy and A. Deák, *Eur. J. Inorg. Chem.* 2014, 4434–4449; (*f*) T. Tunyogi, A. Deák, G. Tárkányi, P. Király and G. Pálinkás, *Inorg. Chem*. 2008, **47**, 2049–2055; (*g*) A. Deák, T. Megyes, G. Tárkányi, P. Király, L. Biczók, G. Pálinkás and P. J. Stang, *J. Am. Chem. Soc.*, 2006, **128**, 12668–12670.

11 (*a*) K. H. Leung, D. L. Phillips, M.-C. Tse, C.-M. Che and V. M. Miskowski, *J. Am. Chem. Soc.*, 1999, **121**, 4799–4803.

12 (*a*) C. Ma, C. T.-L. Chan, W.-P. To, W.-M. Kwok and C.-M. Che, *Chem. Eur. J*. 2015, **21**, 13888–13893; (*b*) W.-F. Fu, K.-C. Chan and K.-K. Cheung and C.-M. Che, *Chem. Eur. J*., 2001, **7**, 4656–4664; (*c*) W.-F. Fu, K.-C. Chan, V. M. Miskowski and C.-M. Che, *Angew. Chem. Int. Ed.*, 1999, **38**, 2783–2785; (*d*) A. L. Balch, *Angew. Chem. Int. Ed.*, 2009, **48**, 2641–2644; (*e*) J. Liang, Z. Chen, J. Yin, G.-A. Yu and S. H. Liu, *Chem. Commun*., 2013, **49**, 3567–3569.

13 (*a*) C. H. Woodall, S. Fuertes, C. M. Beavers, L. E. Hatcher, A. Parlett and H. J. Shepherd, et al. *Chem. Eur. J.* 2014, **20**, 16933–16942; (*b*) B.-C. Tzeng, A. Chao, *Chem. Eur. J.* 2015, **21**, 2083–2089.

14 (*a*) H. Ito, M. Muromoto, S. Kurenuma, S. Ishizaka, N. Kitamara, H. Sato and T. Seki, *Nat. Commun.*, 2013, **4**, 2009; (*b*) T. Seki, K. Sukurada and H. Ito, *Angew. Chem. Int. Ed.* 2013, **52**, 12828–12832; (*c*) T. Seki, T. Ozaki, T. Okura, K. Asakura, A. Sakon, H. Uekusa and H. Ito, *Chem. Sci.* 2015, **6**, 2187–2195; (*d*) R. J. Roberts, N. Bélanger-Desmarais, C. Reber and D. B. Leznoff, *Chem. Commun*., 2014, **50**, 3148–3150; (*e*) F. Baril-Robert, M. A. Radtke and C. Reber, *J. Phys. Chem. C,* 2012, **116**, 2192–2197; (*f*) Z. Assefa, M. A. Omary, B. G. McBurnett, A. A. Mohamed, H. H. Patterson, R. J. Staples and J. P. Fackler, *Inorg. Chem.*, 2002, **41**, 6274–6280.

15 (*a*) H. Schmidbaur and A. Schier, *Chem. Soc. Rev.*, 2008, **37**, 1931–1951; (*b*) H. Schmidbaur and A. Schier, *Chem. Soc. Rev.*, 2012, **41**, 370–412; (*c*) D. M. P. Mingos, *J. Chem. Soc., Dalton Trans*. **1996**, 561–566; (*d*) A. Laguna (Ed.), *Modern Supramolecular Gold Chemistry*, Wiley-VCH, Weinheim, Germany, 2008.

16 (*a*) M. C. Lagunas, C. M. Fierro, A. Pintado-Alba, H. de La Riva and S. Betanzos-Lara, *Gold Bull.*, 2007, **40**, 135–141; (*b*) C.-M. Che, S.-W. Lai, *Coord. Chem Rev.*, 2005, **249**, 1296-1309; (*c*) C. Ma, C.T.-L. Chan, W.-P. To, W.-M. Kwok and C-M Che, *Chem. Eur. J.*, 2015, **21**, 13888–13893.

17 (*a*) F. Mendizabal and S. Miranda-Rojas and L. Barrientos-Poblete, *Comp. Theor. Chem*., 2015, **1057**, 74–79; (*b*) Y. Zhao and D. G. Truhlar, *Theor. Chem. Acc.*, 2008, **120**, 215-241; (*c*) M. J. Frisch, G. W. Trucks, H. B. Schlegel, G. E. Scuseria, M. A. Robb, J. R. Cheeseman, G. Scalmani, V. Barone, B. Mennucci, G. A. Petersson, H. Nakatsuji, M. Caricato, X. Li, H. P. Hratchian, A. F. Izmaylov, J. Bloino, G. Zheng, J. L. Sonnenberg, M. Hada, M. Ehara, K. Toyota, R. Fukuda, J. Hasegawa, M. Ishida, T. Nakajima, Y. Honda, O. Kitao, H. Nakai, T. Vreven, J. A. Montgomery, Jr. , J. E. Peralta, F. Ogliaro, M. Bearpark, J. J. Heyd, E. Brothers, K. N. Kudin, V. N. Staroverov, R. Kobayashi, J. Normand, K. Raghavachari, A. Rendell, J. C. Burant, S. S. Iyengar, J. Tomasi, M. Cossi, N. Rega, J. M. Millam, M. Klene, J. E. Knox, J. B. Cross, V. Bakken, C. Adamo, J. Jaramillo, R. Gomperts, R. E. Stratmann, O. Yazyev, A. J. Austin, R. Cammi, C. Pomelli, J. W. Ochterski, R. L. Martin, K. Morokuma, V. G. Zakrzewski, G. A. Voth, P. Salvador, J. J. Dannenberg, S. Dapprich, A. D. Daniels, ©. Farkas, J. B. Foresman, J. V. Ortiz, J. Cioslowski and D. J. Fox, GAUSSIAN 09 (Revision C.01), Gaussian Inc., Wallingford, CT, 2009.

18 (*a*) A. Pintado-Alba, H. de la Riva, M. Nieuwhuyzen, D. Bautista, P. R. Raithby, H. A. Sparkes, S. J. Teat and J. M. López-de-Luzuriaga and M. C. Lagunas, *Dalton Trans*., 2009, 3459–3467; (*b*) K. H. Leung, D. L. Phillips, Z. Mao, C.-M. Che, V. M. Miskowski and C.-K. Chan, *Inorg. Chem.*, 2002, **41**, 2054–2059.

19 (*a*) Z. Assefa, B. G. McBurnett, R. J. Staples, and J. P. Fackler, *Inorg. Chem.*, 1995, **34**, 4965–4972; (*b*) F. White, L. N. Pham, K. R. Xiang, R. Thomas, P. Vogel, C. Crawford, Z. Assefa, R. E. Sykora, *Inorg. Chim. Acta*, 2014, **414**, 240–249; (*c*) R. B. Thomas, P. A. Smith, A. Jaleel, P. Vogel, C. Cawford, Z. Assefa and R. E. Sykora, *Inorg. Chem.*, 2012, **51**, 3399–3408; (*d*) M. A. Rawashdeh-Omary, J. M. López-de-Luziriaga, M. D. Rashdan, O. Elbjeirami, M. Monge, M. Rodríguez-Castillo and A. Laguna, *J. Am. Chem. Soc.*, 2009, **131**, 3824–3825; (*e*) Y.-A. Lee, J. E. McGarrah, R. J. Lachicotte and R. Eisenberg, *J. Am. Chem. Soc.*, 2002, **124**, 10662–10663.

20 (*a*) M. A. Rawashdeh-Omary, M. A. Omary, H. H. Patterson and J. P. Fackler, *J. Am. Chem. Soc.*, 2001, **123**, 11237–11247; (*b*) G. Cui, X.-Y. Cao, W.-H. Fang, M. Dolg and W. Thiel, *Angew.*

Chem. Int. Ed., 2013, **52**, 10281–10285; (*c*) K. H. Kim, J. G. Kim, S. Nozawa, T. Sato, K. Y. Oang, T. W. Kin, et al. *Nature*, 2015, **518**, 385–389; (*d*) T. Seki, K. Sakurada, M. Muromoto, H. Ito, *Chem. Sci.*, 2015, **6**, 1491–1497.

21 (*a*) Q. Xiao, J. Zheng, M. Li, S.-Z. Zhan, J.-H. Wang and D. Li, *Inorg. Chem.*, 2014, **53**, 11604–11615; (*b*) Q. Benito, X. F. Le Goff, S. Maron, A. Fargues, A. Garcia, C. Martineau, F. Taulelle, S. Kahlal, T. Gacoin, J.-P. Boilot and S. Perruchas, *J. Am. Chem. Soc.* **2014**, 136, 11311–11320; (*c*) S. Perruchas, X. F. le Goff, S. Maron, I. Maurin, F. Guillen, A. Garcia, T. Gacoin and J.-P. Boilot, *J. Am. Chem. Soc.* **2010**, 132, 10967–10969.

22 A. Han, P. Du, Z. Sun, H. Wu, H. Jia, R. Zhang, Z. Liang, R. Cao, R. Eisenberg, *Inorg. Chem.*, 2014, **53**, 3338–3344.

23 (*a*) C. L. van Oosten, C. W. M. Bastiaansen, D. J. Broer, *Nat. Mater.*, 2009, **8**, 677–682. (*b*) J. Park, L.-B. Sun, Y.-P. Chen, Z. Perry, H.-C. Zhou, *Angew. Chem. Int. Ed.*, 2014, **53**, 5842–5846.

24 H. Xiang, J. Cheng, X. Ma, X. Zhou and J. J. Chruma, *Chem. Soc. Rev.*, 2013, **42**, 6128–6185.